Novel DNA Intercalators Based on the Pyridazino[1′,6′:1,2]pyrido[4,3-*b*]indol-5-inium System

Andrés Molina,[†] Juan J. Vaquero,[†] José L. Garcia-Navio,[†] Julio Alvarez-Builla,*[,†,⊥] Beatriz de Pascual-Teresa,[‡,||] Federico Gago,[‡] and María M. Rodrigo[§]

Departamento de Química Orgánica, Departamento de Farmacología, and Departamento de Química-Física, Universidad de Alcalá, 28871-Alcalá de Henares, Madrid, Spain

Received November 5, 1998

A new class of DNA intercalators based on the *8H*-pyridazino[1′,6′:1,2]pyrido[4,3-*b*]indol-5-inium system in which the cationic nature of the chromophore is provided by a brigdehead quaternary nitrogen has been obtained. These cations along with 10*H*-indolo[3,2-*c*]pyridazino[1,6-*a*]quinolin-5-inium, 13*H*-dibenz[*f*,*h*]indolo[3′,2′:3,4]pyrido[1,2-*b*]cinnolin-10-inium, and 5*H*-acenaphtho[1′,2′:3′,4′]pyridazino[1′,6′:1,2]pyrido[4,3-*b*]indol-8-inium were synthesized by the Westphal reaction of carbolinium derivatives with various 1,2-dicarbonyl compounds. When these tetra-, penta-, and heptacyclic heteroaromatic nuclei were evaluated as DNA intercalators using UV−vis spectroscopy, viscometric determinations, and unwinding angle determinations, we found that only the 8*H*-pyridazino[1′,6′:1,2]pyrido[4,3-*b*]indol-5-inium cations behaved as DNA intercalators. Molecular modeling studies allowed the preferred orientation of the intercalating chromophore within a CpG intercalation site to be explored and will provide help in the rational design of novel bis-intercalators based on these chromophores.

Introduction

The DNA molecule is the primary target of many antitumor agents.[1] Among the binding modes of drugs to DNA, both intercalative and nonintercalative mechanisms have been described and in both cases a certain degree of sequence selectivity has been shown.[2] The term intercalator[3] is applied to those compounds capable of stacking between the DNA base pairs, thus provoking conformational changes in the double helix with consequences for the normal mechanisms of DNA replication, transcription, and repair.[4] Interference with these functions usually results in nonspecific cell killing[5] with potential applications in the field of antitumor drugs.[1]

Intercalators always contain a planar chromophore with at least two fused π-deficient aromatic rings.[6] The preference most intercalators show for 5′-CpG-3′ steps is supported by ample experimental evidence and is generally attributed to (i) the greater polarizability of G:C pairs relative to A:T pairs,[7] (ii) the larger overlapping surface provided by pyrimidine−purine compared to purine−pyrimidine steps,[8] and (iii) the lower energy required for unstacking this sequence relative to others.[9] Computational chemistry tools have proved their usefulness in our attempts to understand the determinants of specificity involved in the recognition process[10] and can be of further help in the design of new compounds with tailor-made binding properties.

It is also known that the transformation of neutral chromophores to their cationic derivatives usually enhances the affinity of these compounds for DNA (e.g. elliptinium vs ellipticine[11]), thus improving their antitumor activity.[12] Most current cationic intercalators belong to the class of *N*-alkyl azinium salts,[13] one of the two general types of polycyclic aromatic nitrogen cations (Chart 1). Surprisingly, the DNA intercalating properties of the other type, the quinolizinium salts, remain largely unexplored.[14]

As a result of these considerations, we have initiated a program focused on exploring different heterocycles as

† Departamento de Química Orgánica.
‡ Departamento de Farmacología.
§ Departamento de Química-Física.
⊥ FAX: 34-1-918854660. E-mail: jalvarez@quimor.alcala.es.
|| Current address: Departamento de Química, Universidad San Pablo CEU, E-28668 Madrid.

(1) (a) *Cancer Chemotherapeutic Agents*; Foye, W. O., Ed..; American Chemical Society: Washington, D.C., 1995. (b) *Nucleic Acid Targeted Drug Design*; Propst, C. L., Perun, T. L., Eds.; Marcel Dekker: New York, 1992. (c) *Molecular Aspects of Anti-cancer Drug Action*; Neidle, S., Waring, M. J., Eds.; MacMillan: London, 1983.

(2) Krugh, T. R. *Curr. Op. Str. Biol.* **1994**, *4*, 351.

(3) (a) For pioneering works on intercalation, see: (a) Lerman, L. S. *J. Mol. Biol.* **1961**, *3*, 18. (b) Lerman, L. S. *Proc. Natl. Acad. Sci. U.S.A.* **1963**, *49*, 94.

(4) Wilson, W. D.; Jones, R. In *Intercalation Chemistry*; Whittingham, M. S., Jacobson, A. J., Eds.; Academic Press: New York, 1981; Chapter 14.

(5) Denny, W. A.; Baguley, B. C.; Cain, B. F.; Waring, M. J. In *Mechanism of Action of Anticancer Drugs*; Neidle, S., Waring, M. J., Eds.; MacMillan: London, 1983.

(6) Miller, K. J.; Newlin, D. D. *Biopolymers* **1982**, *21*, 633.

(7) (a) Müller, W.; Crothers, D. M. *Eur. J. Biochem.* **1975**, *54*, 267. (b) Krugh, T. R.; Reinhardt, C. G. *J. Mol. Biol.* **1975**, *97*, 133.

(8) Day, R. O.; Seeman, N. C.; Rosenberg, J. M.; Rich, A. *Proc. Natl. Acad. Sci. U.S.A.* **1973**, *70*, 849.

(9) (a) Ornstein, R. L.; Rein, R.; Breen, D. L.; MacElroy, R. D. *Biopolymers* **1978**, *17*, 2341. (b) Nuss, M. E.; Marsh, F. J.; Kollman, P. A. *J. Am. Chem. Soc.* **1979**, *101*, 825.

(10) (a) Gallego, J.; Luque, F. J.; Orozco, M.; Burgos, C.; Alvarez-Builla, J.; Rodrigo, M. M.; Gago, F. *J. Med. Chem.* **1994**, *37*, 1602. (b) Gallego, J.; Luque, F. J.; Orozco, M.; Gago, F. *J. Biomol. Struct. Dyn.* **1994**, *12*, 11. (c) de Pascual-Teresa, B.; Gallego, J.; Ortiz, A. R.; Gago, F. *J. Med. Chem.* **1996**, *39*, 4810. (d) Gallego, J.; Ortiz, A. R.; Pascual-Teresa, B.; Gago, F. *J. Comput.-Aided Mol. Design* **1997**, *11*, 114. (e) Pastor, J.; Siro, J. G.; García Navio, J. L.; Vaquero, J. J.; Alvarez-Builla, J.; Gago, F.; Pascual-Teresa, B.; Pastor, M.; Rodrigo, M. *J. Org. Chem.* **1997**, *62*, 5476.

(11) (a) Kansal, V. K.; Potier, P. *Tetrahedron* **1986**, *42*, 2389. (b) Gribble, G. W. The Alkaloids; Brossi, A.; Ed.; Academic Press: 1990; Vol. 39, p 239.

(12) Waring, M. J. *J. Mol. Biol.* **1970**, *54*, 247.

(13) Pons, M.; Campayo, L.; Martinez-Balbas, M. A.; Azorin, F.; Navarro, P.; Giralt, E. *J. Med. Chem.* **1991**, *34*, 82.

(14) For the two reported examples, see: (a) Caprasse, M.; Houssier, C. *Biochemie* **1984**, *66*, 31. (b) Feigon, J.; Denny, W. A.; Leupin, W.; Dearns, D. V. *J. Med. Chem.* **1984**, *27*, 450.

10.1021/jo982216d CCC: $18.00
Published on Web 05/06/1999

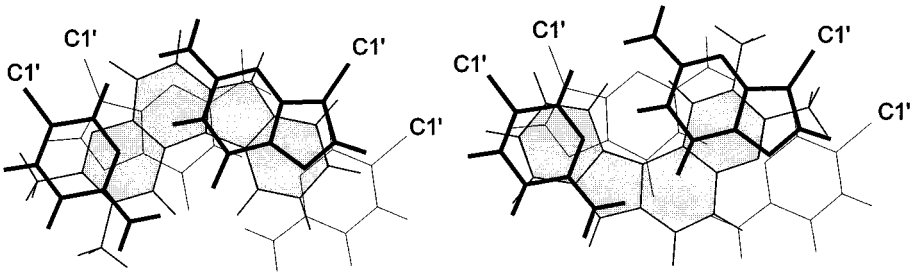

Figure 1. Schematic representation of chromophore **3a** intercalated into the DNA dimer $d(CG)_2$ with the convex edge in the minor groove (left; complex **m**) or the major groove (right; complex **M**).

Chart 1

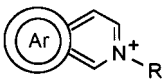

DNA intercalators N-alkyl azinium type

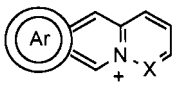

DNA intercalators quinolizium type

Ar = aromatic; X = CH, N

candidates for transformation into polycyclic aromatic cations bearing a bridgehead quaternary nitrogen atom.[10e,15] The present work reports on one of these quinolizinium-type systems based on γ-carboline. From this system different polycyclic azonia derivatives were built, some of which were shown to behave as DNA intercalators. Ab initio molecular orbital methods have been used to calculate the molecular electrostatic potentials of these intercalators and to assign point charges to their constituent atoms.

To introduce rational modifications into these chromophores and achieve successful bis-intercalators[16] it was essential to gain insight into the principles that dictate binding orientation. To this end, molecular modeling and molecular dynamics techniques have been employed to explore the more favorable orientation of the chromophore between the base pairs.

Computational Methods

Ring systems **3a**−**f** were model-built using standard bond lengths and angles and the Insight II program.[17] The initial goemetries were fully optimized by means of the ab initio quantum mechanical program Gaussian 92[18] and the 3-21G basis set. Single-point calculations using the larger 6-31G* basis set on the optimized RHF/3-21G geometries were then carried out in order to calculate point charges which could accurately reproduce the molecular electrostatic potential.[19] The AMBER[20] all-atom force field parameters were used for the molecular mechanics calculations. Covalent parameters for the chromophores were derived, by analogy or through interpolation, from those already present in the AMBER database.

The complex of ellipticine with 5-iodocytidylyl-(3′-5′)-guanosine[21] was retrieved from the Cambridge Structural Database (ref. EICGUA) and used as a template for modeling a $d(CG)_2$ dinucleotide step ready for intercalation. Two different complexes were then constructed by inserting the simplest chromophore **3a** into this intercalation site (hereafter referred to as CpG) in the two possible orientations relative to the base pairs (Figure 1). Electrical neutrality was achieved by placing a hydrated counterion in the bisector of the phosphate group located further from the positive charge of the ligand.

The initial complexes were refined by performing 5000 steps of steepest descent energy minimization in a continuum medium of relative permittivity $4r_{ij}$ using a cutoff of 10 Å for the nonbonded interactions. The systems were then subjected to molecular dynamics simulations under the same conditions. The temperature was weakly coupled to a thermal bath[22] with a relaxation time of 0.1 ps; in a 5 ps heating phase, the temperature was raised to 300 K in steps of 10 K over 0.1 ps blocks, the velocities being reassigned according to a Maxwell−Boltzmann distribution at each new temperature. This was followed by an equilibration phase of 15 ps at 300 K, in which the velocities were reassigned in the same way every 0.2 ps during the first 5 ps, and by a 80 ps sampling period during which system coordinates were saved every 0.2 ps. The time step used was 1 fs in the heating period and 2 fs during the rest of the simulations. All bonds involving hydrogens were constrained to their equilibrium values by means of the SHAKE algorithm,[23] and the lists of nonbonded pairs were updated every 25 steps. For the initial 30 ps, selected sugar−phosphate backbone atoms were restrained to their reference positions in Cartesian space by means of a harmonic force constant of 10 kcal mol^{-1} $Å^{-2}$. For the whole length of the simulations, all possible hydrogen bonds between DNA bases were restrained by use of harmonic force constants of 50 kcal mol^{-1} $Å^{-2}$ and 50 kcal mol^{-1} rad^{-2} for distances and angles, respectively.

Both the geometries of the complexes and the DNA−ligand interaction energies were monitored and analyzed using the 400 coordinate sets collected during the last 80 ps of the molecular dynamics simulations. The energy analyses were performed using a dielectric constant of 1 for the electrostatic interactions and a cutoff distance of 10 Å. The stacking

(15) (a) Molina, A.; Vaquero, J. J.; García Navío, J. L.; Alvarez-Builla, J.; Rodrigo, M. M.; Castaño, O.; Andrés, J. L. J. *Bioorg. Med. Chem. Lett.* **1996**, *13*, 1453. (b) Pastor, J.; Siró, J.; García Navío, J. L.; Vaquero, J. J.; Rodrigo, M. M.; Ballesteros, M.; Alvarez-Builla, J. *Bioorg. Med. Chem. Lett.* **1995**, *5*, 3043. (c) Santiesteban, I.; Siro, J. G.; Vaquero, J. J.; García-Navio, J. L.; Alvarez-Builla, J.; Castaño, O.; Andrés, J. L. *J. Org. Chem.* **1995**, *60*, 5667.

(16) For a review on bis-intercalators, see: Wakelin, L. P. G. *Med. Chem. Rev.* **1986**, *6*, 275.

(17) Insight II, release 95.0, 1995, Biosym/Molecular Simulations, 9685 Scranton Road, San Diego, CA 92121-3752.

(18) Gaussian 92, Revision D.2, Frisch, M. J.; Trucks, G. W.; Head-Gordon, M.; Gill, P. M. W.; Wong, M. W.; Foresman, J. B.; Johnson, G.; Schlegel, H. B.; Robb, M. A.; Replogle, E. S.; Gomperts, R.; Andres, J. L.; Raghavachari, K.; Binkley, J. S.; González, C.; Martin, R. L.; Fox, D. J.; Defrees, D. J.; Baker, J.; Stewart; J. J. P.; Pople, J. A. Gaussian, Inc., Pittsburgh, PA, 1992.

(19) Besler, B. H.; Mertz, K. M. Jr.; Kollman P. A. *J. Comput. Chem.* **1990**, *11*, 431.

(20) (a) AMBER version 4.0. Pearlman, D. A.; Case, D. A.; Caldwell, J.; Seibel, G.; Singh, U. C.; Weiner, P.; Kollman, P. A. Department of Pharmaceutical Chemistry, University of California, San Francisco, 1991. (b) Weiner, S. J.; Kollman, P. A.; Nguyen, D. T.; Case, D. A. *J. Comput. Chem.* **1986**, *7*, 230.

(21) Jain, S. C.; Bhandary, K. K.; Sobell, H. M. *J. Mol. Biol.* **1979,** *135*, 813.

(22) Berendsen, H. J. C.; Postma, J. P. M.; van Gusteren, W. F.; DiNola, A.; Haak, J. R. *J. Chem. Phys.* **1984**, *81*, 3684.

(23) Ryckaert, J. P.; Ciccoti, G.; Berendsen, H. J. C. *J. Comput. Phys.* **1977**, *23*, 327.

Scheme 1

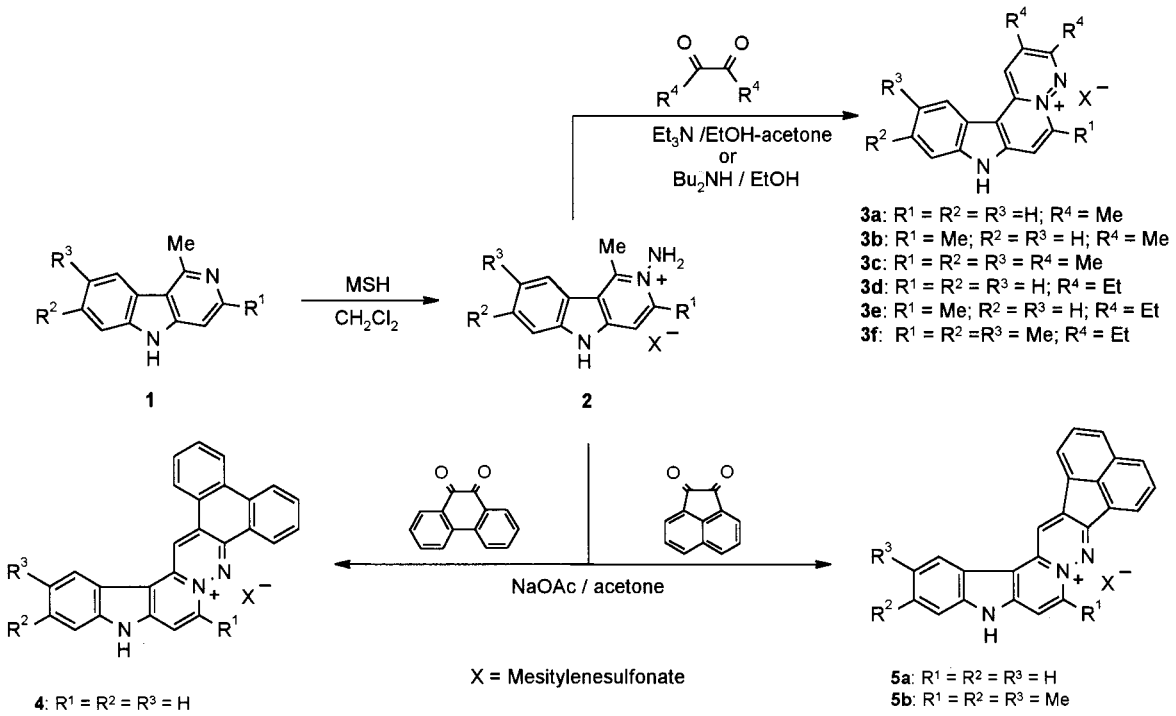

Scheme 2

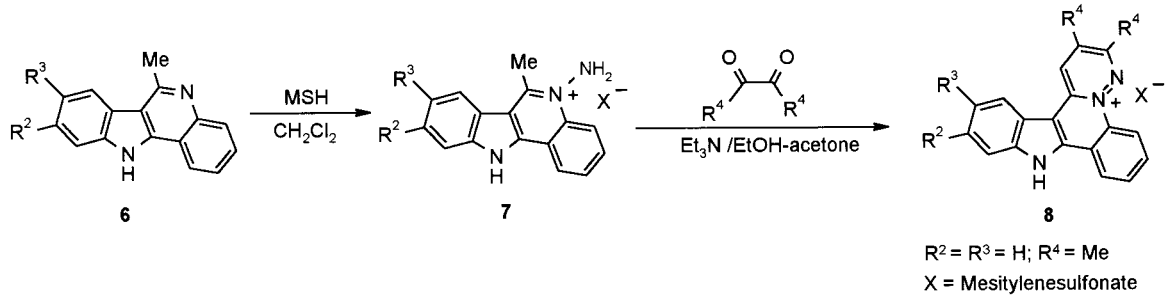

energies were calculated between the chromophore and the nucleobases using the deoxyribose C1′ atoms as buffers in order to achieve electrical neutrality.[10c,24]

On the basis of the results obtained for compound **3a** (see below), only the orientation which locates the convex side of the chromophore in the minor groove (complex **m** in Figure 1) was considered for the rest of the ligands.

Results and Discussion

Synthesis. The 1-methyl-γ-carbolines **1**, chosen as models for the preparation of nonlinearly fused cations, were prepared either by thermal or microwave decomposition of the corresponding pyridylbenzotriazoles (Graebe−Ullmann reaction)[25,26] as previously described.[27] These derivatives were easily transformed into the salts **2** by amination with (*O*-mesitylenesulfonyl)hydroxylamine (MSH) in CH_2Cl_2 at room temperature. The reaction of **2** with various 1,2-dicarbonyl compounds (Westphal condensation)[28,29] afforded several types of azonia derivatives although different reaction conditions were necessary for the condensation to be successful (Scheme 1). Thus, to obtain the polycyclic cations **4** and **5** from the reaction of **2** with 1,2-acenaphthenequinone and 9,10-phenanthrenequinone, the condensation had to be carried out in sodium acetate/acetone whereas in the reaction of **2** with 2,3-butanedione or 3,4-hexanedione **3a**−**e** could only be obtained if triethylamine/MeOH/acetone was employed. The synthesis of the cation **3f** required the use of *n*-dibutylamine/EtOH.

Analogously, the amination of the benzo-γ-carboline **6** obtained by reaction of 4-chloroquinoline and pyridylbenzotriazole[27] afforded the *N*-amino carbolinium salt **7** which condensed with 3,4-hexanedione to yield the pentacyclic cation **8** (Scheme 2).

DNA Binding Studies. Several techniques were used to evaluate the DNA binding properties[30] of compounds **3**−**5** and **8**. It was not possible to obtain accurate data

(24) Gallego, J.; Ortiz, A. R.; Gago, F. *J. Med. Chem.* **1993**, *36*, 1548.
(25) Graebe, C.; Ullman, F. *Justus Liebigs Ann. Chem.* **1896**, *291*, 16.
(26) For examples, see: (a) Laurson, W.; Perkin, W. H.; Robinson, R. *J. Chem. Soc.* **1924**, *125*, 626. (b) Freak, R. H.; Robinson, R. *J. Chem. Soc.* **1938,** 2013. (c) Kaczmarek, L.;. Balicki, R.; Nantka-Namirski, P. *Arch. Pharm.* **1988**, *321*, 463. (c) Parrick, J.; Yahya, J. *J. Chem. Res., Synop.* **1990**, 1; *J. Chem. Res., Miniprint* **1990**, 201. (d) Mehta, L. K.; Parrick, J.; Payne, F. *J. Chem. Soc., Perkin Trans. 1* **1993**, 1261.
(27) Molina, A.; Vaquero, J. J.; García Navío, J. L.; Alvarez-Builla, J.; Pascual-Teresa, B.; Gago, F.; Rodrigo, M. M.; Ballesteros, M. *J. Org. Chem.* **1996**, *61*, 5587.
(28) Westphal, O.; Jahn, K.; Heffe, W. *Arch. Pharm.* **1961**, *294*, 37.
(29) For other examples, see: (a) Diaz, A.; Matia, M. P.; García-Navío, J. L.; Vaquero, J. J.; Alvarez-Builla, J. *J. Org. Chem.* **1994**, *59*, 8294. (b) Matía, M. P.; García Navío, J. L.; Vaquero, J. J.; Alvarez-Builla, J. *Liebigs Ann. Chem.* **1992**, 777.

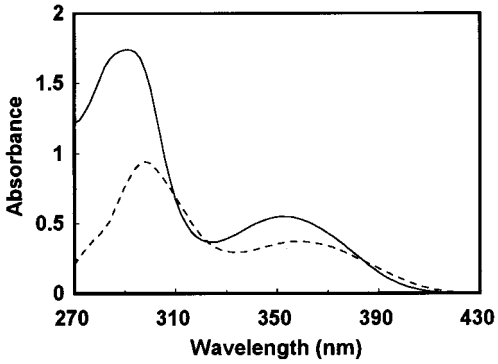

Figure 2. Effect of calf thymus DNA on the ultraviolet absorption spectrum of **3a** in Tris-HCl (pH = 7.5). Solid lines indicate spectrum of **3a** alone at a concentration of 4.12×10^{-6} M, and dashed lines represent the spectrum of **3a** at the same concentration in the presence of 9.71×10^{-5} M DNA (nucleotide molarity).

for compound **8** because of its low solubility. Addition of compounds **4** and **5** to a sample of sonicated calf thymus DNA in Tris-HCl (pH = 7.5) induced hyperchromicity, probably due to dipole−dipole interactions, indicating the absence of complex formation between these cations and DNA. However, the derivatives **3** showed characteristic changes in their visible absorption spectra as a result of complex formation. Both hypochromic and bathochromic shifts between 10 and 16 nm relative to the spectra of the free compounds[31] were observed (Figure 2). Composite spectra exhibit well-defined isosbestic points for this series, which is indicative of two distinct absorbing species (free and bound compound). From the spectral changes, nonlinear Scatchard binding isotherms were generated for the interaction of these compounds with DNA. Each binding isotherm contains data sets from multiple experiments and presents the form shown in Figure 3 for the representative compound **3a**. The points are experimental values and the solid lines the result of nonlinear least-squares regression determinations using the noncooperative McGhee−Von Hippel equation[32] (see Experimental Section) where v is the ligand binding ratio and c is the free compound concentration. The cooperative McGhee−von Hippel model was also used in the analysis of the interaction, but the very low values obtained for ω, the binding cooperativity factor, indicate that the binding in this series is noncooperative. The binding parameters (K, n) determined in this manner for **3a**−**f** are shown in Table 1 , with K being the apparent binding constant and n the number of nucleotides per bound molecule. All derivatives have DNA affinity constant values around 10^5 M^{-1}, which are essentially of the same order of magnitude as that of the well-known intercalator ethidium bromide,[33] used here as a reference and measured under the same conditions (Table 1). The position

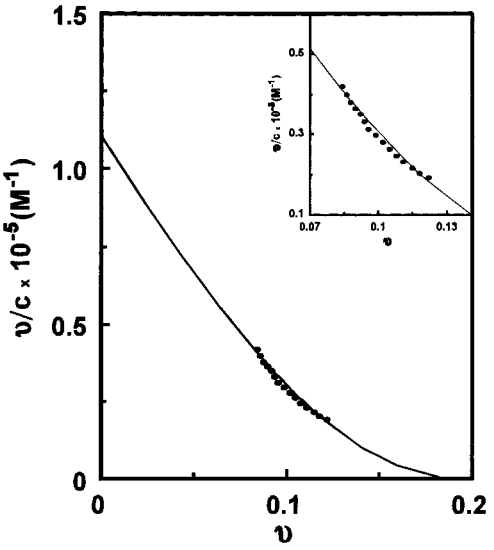

Figure 3. Scatchard plot for the binding of **3a** to calf thymus DNA. Values for binding ratio v (molar ratio of bound compound per DNA nucleotide) and free compound concentration c were determined from data taken from spectrophotometric titrations of the compound by DNA. Points in the figure are the data, and solid lines are the best fits from the noncooperative McGhee−von Hippel model.[32]

Table 1. DNA Binding Properties of Azonia Derivatives 3[a]

compd	R^1	R^2	R^3	R^4	$\Delta\lambda$	H	K	n	m	ϕ
3a	H	H	H	Me	10	36	1.10	4.75	1.16	30
3b	Me	H	H	Me	10	38	0.95	3.85	0.97	ND
3c	Me	Me	Me	Me	16	39	2.39	3.84	NM	NM
3d	H	H	H	Et	10	32	1.27	3.98	0.95	ND
3e	Me	H	H	Et	10	34	2.62	3.56	0.87	ND
3f	Me	Me	Me	Et	10	30	1.45	3.00	0.77	ND
EtBr							2.06	4.38	1.16	26

[a] $\Delta\lambda = (\lambda_{bound} - \lambda_{free})$; λ_{free} and λ_{bound} are wavelength of maximum absorption for free and DNA bound compounds. H = percent hypochromicity [% H = $(1 - \epsilon_{bound}/\epsilon_{free}) \times 100$]. ϵ_{free} and ϵ_{bound} are extinction coefficients for free and DNA bound compounds. K = affinity constant for DNA (10^5 M^{-1}). n = number of nucleotides per bound molecule. m = helix extension slope measured by sonicated DNA viscometric lengthening; values within 0.03−0.25 error. ϕ = unwinding angle of closed circular supercoiled plasmid pBR325. The unwinding angles were determined assuming an unwinding angle of 26° for ethidium eromide. EtBr = ethidium bromide. ND = not determined. NM = not measurable due to weak solubility.

and number of alkyl substituents on the cationic system had only a small effect on the DNA affinities of these chromophores, with **3e** showing the highest value. By replacing the methyl substituents at the C2 and C3 positions of the chromophore with ethyl groups, the DNA binding affinity is moderately enhanced in some cases (**3d** vs **3a** and **3b** vs **3d**) while in others it is slightly decreased (**3f** vs **3c**). Moreover, while in the methylated series (R^4 = Me, **3a**−**c**) the pentaalkylated derivative **3c** shows the highest affinity, the corresponding pentaalkylated derivative **3f** in the ethylated series (R^4 = Et, **3d**−**f**) shows an affinity constant lower than that of the trialkylated compound **3e**.

Unwinding and extension of the DNA backbone in intercalated complexes results in length and viscosity increases in sonicated DNA.[30] When the viscosity of sonicated calf thymus DNA was measured in the absence and presence of increasing concentrations of the cationic compounds **3**, a plot (Figure 4) of the relative increase in contour length, L/L_o, versus the molar ratio of added

(30) For criteria for the mode of binding to DNA, see: (a) Suh, D.; Chaires, J. B. *BioMed Chem*. **1995**, *3*, 723. (b) Long, E. C.; Barton, J. K. *Acc. Chem. Res*. **1990**, *23*, 2773.

(31) Binding commonly results in hypochromism and a shift of the transition to longer wavelength in the intercalated chromophore. (a) Dougherty, G.; Pigram, W. J. *CRC Crit. Rev. Biochem*. **1982**, *12*, 103. (b) Berman, H. M.; Young, P. R. *Annu. Rev. Biophys. Bioeng*. **1981**, *10*, 87.

(32) McGhee, J. D.; von Hippel, P. H. *J. Mol. Biol*. **1974**, *86*, 469.

(33) (a) Fairley, T. A.; Tidwell, R. R.; Donkor, I.; Naiman, N. A.; Ohemeng, K. A.; Lombardy, R. J.; Bentley, J. A.; Cory, M. *J. Med. Chem*. **1993**, *36*, 1746. (b) Cory, M.; Tidwell, R. R.; Fairley, T. A. *J. Med. Chem*. **1992**, *35*, 431. (c) Graves, D. E.; Watkins, C. L.; Yielding, L. W. *Biochemistry* **1981**, *20*, 1887.

Scheme 3

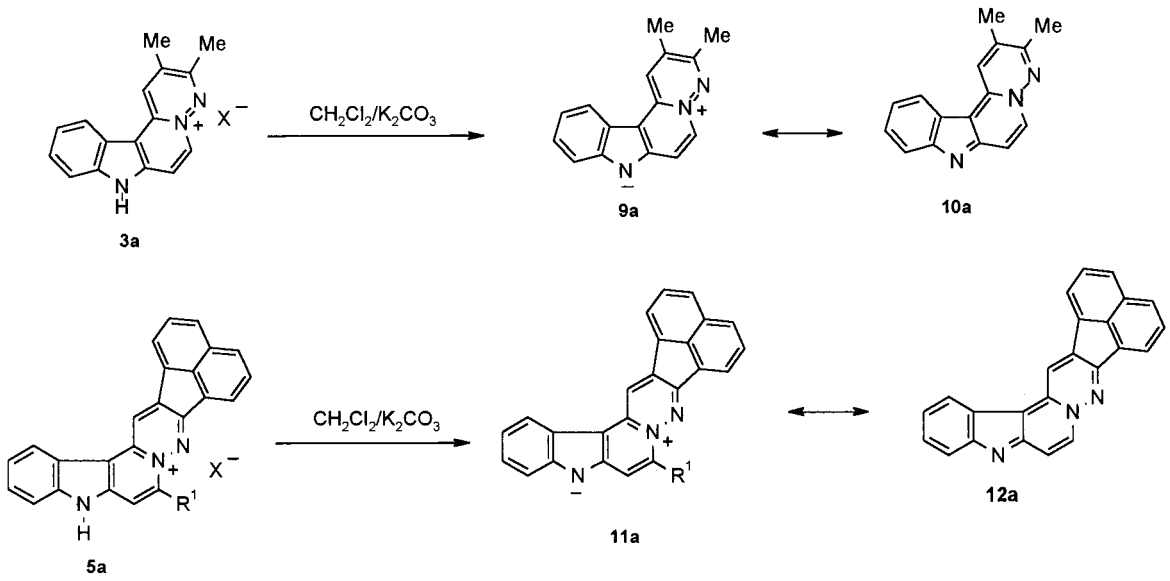

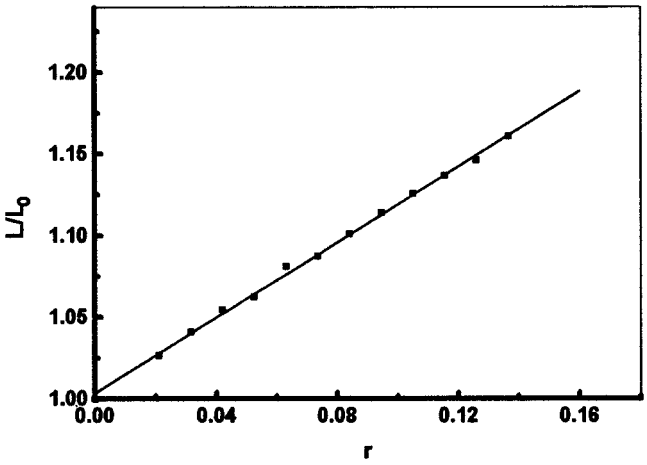

Figure 4. Relative length increase L/L_o of **3a**−DNA complexes as a function of the molar ratio of added compound to DNA nucleotides *r*. The contour lengths in the presence (*L*) or absence (L_o) of the compound were calculated from viscosity measurements on sonicated calf thymus DNA.

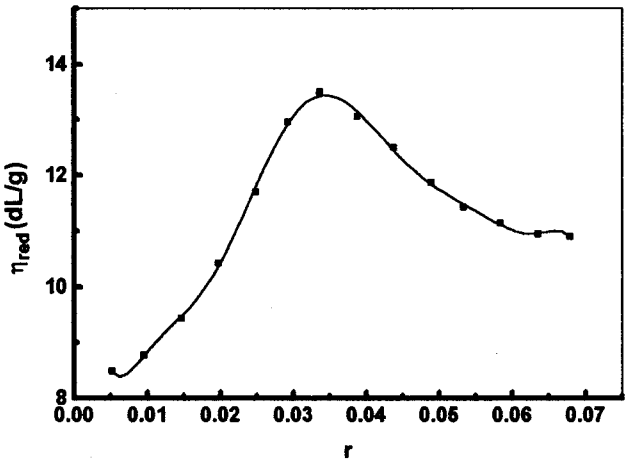

Figure 5. Representative experiments showing unwinding of closed circular supercoiled plasmid pBR325 by compound **3a**.

compound to DNA nucleotides, *r*,[16,34] yielded the slopes *m*, shown in Table 1. Adopting the criterion of Cory,[33,35] based on the pioneering methodology of Cohen and Eisenberg[34] for monofunctional intercalators such as ethidium bromide, proflavine, and the aminoacridines, which usually have values of *m* between 0.8 and 1.5, all derivatives **3** have *m* values which fall within the range for intercalators.

The ability to unwind closed circular supercoiled DNA, which seems to be the most crucial test to prove intercalative binding,[36] was also demonstrated for the representative compound **3a**. Addition of increasing amounts of **3a** to pBR325 DNA caused removal and then reversal of the supercoils (Figure 5) and gave an unwinding angle of 30° for this compound, a value which is characteristic of intercalating ligands,[36b,37] leaving no doubt as to the DNA intercalative binding ability of the pyridazino[1',6':1,2]pyrido[4,3-*b*]indol-5-inium chromophore.

The question of whether the cationic species **3** or the corresponding deprotonated forms **9** predominate in the buffers used was addressed by determining the pK_a of **3a** as a representative member of the series. The value of 6.8 obtained implies that at the pH of the buffer (pH = 7.5) the deprotonated form must be significantt. In fact, when salts **3a** and **5a** were deprotonated in the two-phase system CH_2Cl_2/K_2CO_3, we were able to isolate the corresponding heterobetaines **9a** and **11a**, respectively, which can be better represented as the covalent forms **10a** and **12a** (anhydrobases) (Scheme 3). When **9a** was subjected to the same spectrophotometric titrations as those described for the corresponding salt **3a**, identical results were observed for both UV values and DNA binding constants.

Molecular Modeling. The evidence that the tetracyclic derivatives **3** are intercalated upon binding to DNA

(34) (a) Cohen, G.; Eisenberg, H. *Biopolymers* **1966**, *4*, 429. (b) Cohen, G.; Eisenberg, H. *Biopolymers* **1969**, *8*, 45.

(35) Cory, M.; Mckee, D. D.; Kagan, J.; Henry, D. W.; Miller, J. A. *J. Am. Chem. Soc.* **1985**, *107*, 2528.

(36) (a) Zimmerman, S. C.; Lamberson, C. R.; Cory, M.; Fairley, T. A. *J. Am. Chem. Soc.* **1989**, *11*, 6805. (b) McKenna, R.; Beveridge, A. J.; Jenkins, T. C.; Neidle, S.; Denny, W. A. *Mol. Pharmacol.* **1989**, *35*, 720. (c) Révet, B. M. J.; Schmir, M.; Vinograd, J. *Nature (London) New Biol.* **1971**, *229*, 10.

(37) Wakelin, L. P. G.; Waring, M. J. *Biochem. J.* **1977**, *157*, 721.

Table 2. Ab Initio 6-31G*\\3-21G Electrostatic Potential Atomic Charges[a] for Chromophores 3a−f

3a		3b		3c		3d		3e		3f	
C1	−0.208	C1	−0.235	C1	0.094	C1	0.139	C1	−0.175	C1	−0.078
H1	0.199	H1	0.207	H1	0.160	H1	0.182	H1	0.193	H1	0.172
C2	0.049	C2	0.106	C2	0.016	C2	−0.131	C2	−0.076	C2	−0.147
Me2	0.031	Me2	0.032	Me2	0.038	Et2	0.144	Et2	0.134	Et2	0.158
C3	0.634	C3	0.499	C3	0.577	C3	0.518	C3	0.420	C3	0.445
Me3	−0.006	Me3	0.011	Me3	−0.008	Et3	0.090	Et3	0.092	Et3	0.094
N4	−0.594	N4	−0.456	N4	−0.510	N4	−0.590	N4	−0.437	N4	−0.471
N5	0.300	N5	0.121	N5	0.241	N5	0.407	N5	0.134	N5	0.197
C6	0.019	C6	0.394	C6	0.324	C6	−0.086	C6	0.338	C6	0.337
H6	0.209	Me6	0.034	Me6	−0.038	H6	0.228	Me6	0.053	Me6	0.040
C7	−0.455	C7	−0.576	C7	−0.450	C7	−0.410	C7	−0.555	C7	−0.523
H7	0.260	H7	0.274	H7	0.255	H7	0.252	H7	0.267	H7	0.264
C7a	0.023	C7a	0.057	C7a	0.057	C7a	0.115	C7a	0.203	C7a	0.059
N8	−0.557	N8	−0.570	N8	−0.333	N8	−0.573	N8	−0.583	N8	−0.461
H8	0.415	H8	0.419	H8	0.370	H8	0.420	H8	0.421	H8	0.391
C8a	0.296	C8a	0.293	C8a	0.087	C8a	0.269	C8a	0.248	C8a	0.230
C9	−0.319	C9	−0.334	C9	−0.334	C9	−0.294	C9	−0.292	C9	−0.456
H9	0.209	H9	0.211	H9	0.208	H9	0.201	H9	0.205	H9	0.239
C10	−0.070	C10	−0.041	C10	0.168	C10	−0.084	C10	−0.093	C10	0.225
H10	0.170	H10	0.161	Me10	0.017	H10	0.169	H10	0.169	Me10	−0.003
C11	−0.182	C11	−0.197	C11	0.134	C11	−0.161	C11	−0.143	C11	0.152
H11	0.177	H11	0.177	Me11	−0.005	H11	0.171	H11	0.170	Me11	−0.015
C12	−0.205	C12	−0.206	C12	−0.387	C12	−0.256	C12	−0.307	C12	−0.400
H12	0.180	H12	0.175	H12	0.230	H12	0.196	H12	0.199	H1	0.226
C12a	0.459	C12a	0.493	C12a	0.207	C12a	0.486	C12a	0.531	C12a	0.394
C12b	−0.182	C12b	−0.263	C12b	−0.007	C12b	−0.308	C12b	−0.416	C12b	−0.204
C12c	0.147	C12c	0.213	C12c	−0.001	C12c	0.184	C12c	0.299	C12c	0.136

[a] Me and Et stand for the whole of the methyl or ethyl substituents, respectively.

led us to explore the preferred orientation of the chromophore within a typical intercalation site. This knowledge can be crucial when designing bis-intercalators as it can suggest the best site of attachment to the chromophore of a linking chain of optimal length whose nature can be varied depending on whether it will be located in either the minor or the major groove.

Electrostatic potential charges for chromophores **3a**−**f** were calculated using ab initio techniques (6-31G*\\3-21G basis set) and are shown in Table 2. On the basis of earlier work,[10,24] our hypothesis was that electrostatics should largely dictate the orientational preferences of these chromophores with respect to the highly polarized G:C base pairs that make up the intercalation site. Two alternate orientations within a typical intercalation step, initially related to each other by approximately a 180° rotation (Figure 1), were investigated for **3a**, taken as a representative compound of the series. After about 50 ps of molecular dynamics simulations, both complexes are virtually undistinguishable (Figure 6) as the chromophore becomes "locked" in a position such that its convex side is located in the minor groove, irrespective of the initial geometry. This orientation does not change for the remaining part of the simulations as it is stabilized by a combination of steric interactions involving the methyl groups and electrostatic interactions emanating from the distinctive charge distribution on the heteroaromatic ring system and the DNA base pairs.[38]

Only this preferred orientation was considered for ligands **3b**−**f**, and it was maintained throughout the molecular dynamics simulations. No significant differences were observed between methylated (**3a**−**c**) and ethylated series (**3d**−**f**), whereas methylation at positions

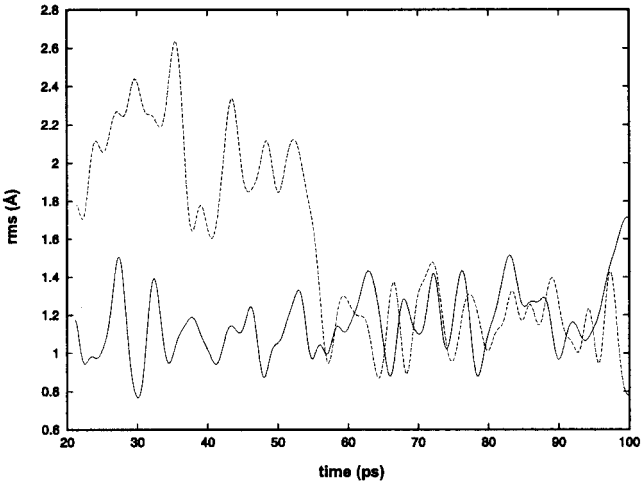

Figure 6. Evolution of the root-mean-square deviation (calculated for all non-hydrogen atoms after least-squares fitting of the structures using the same atoms) from the corresponding refined initial structure of complex **m** (solid lines) along the sampling period of the molecular dynamics simulations. Note the sharp decrease in rmsd in the simulation of complex **M** (dashed lines) after 50 ps resulting from a 180° rotation of the chromophore relative to the bases so as to share the orientation found in complex **m** (convex edge in the minor groove), which was maintained for the remainder of the simulation.

C-10 and C-11 (**3c** and **3f**) was found to result in more favorable and less fluctuating interaction energies (Figure 7).

Conclusions

New pyridazino[1′,6′:1,2]pyrido[4,3-*b*]indol-5-inium cations have been prepared which are able to bind to DNA through intercalation, as demonstrated by UV−visible, spectrophotometry, viscometric titrations, and unwinding of supercoiled pBR325-DNA.

It is also seen that, despite the shortcomings inherent in performing the theoretical calculations in the absence

(38) (a) Gallego, J.; Pascual-Teresa, B.; Ortiz, A. R.; Pisabarro, M. T.; Gago, F. In *QSAR and Modelling: Concepts, Computational Tools and Biological Applications*; Sanz, F., Giraldo, J., Manaut, F., Eds.; J. R. Prous: Barcelona, 1995; pp 274−281. (b) Gago, F. *Methods: A Companion to Methods in Enzymology* **1998**, *14*, 277.

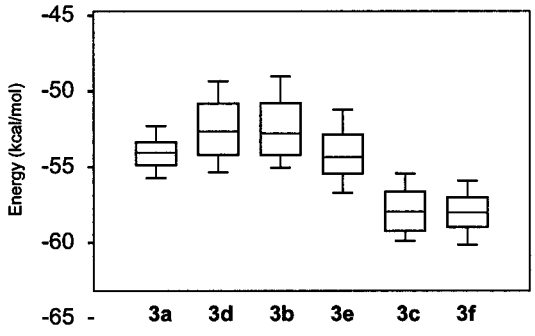

Figure 7. Box plot showing the median (line across the middle of each box), 25th and 75th percentiles (edges of the box), and 10th and 90th percentiles (lower and upper lines, respectively) of the total DNA−ligand interaction energies (kcal mol^{-1}) in the intercalated complexes **3a**−**f** with $d(CG)_2$ during the 20−100 ps period of the molecular dynamics simulations.

of explicit solvent molecules, the present results support the view[10] that the orientational preferences of an intercalating chromophore may have important effects on complex stability. These preferences, which arise from both van der Waals and electrostatic forces, can likely be modulated through functionalization and can be used to advantage in the design of novel bis-intercalators.

Validation of these preliminary theoretical models will have to await the results of NMR studies with oligonucleotides of known sequence. Work is currently underway in order to select a suitable oligonucleotide from DNA random sequence libraries using in vitro selection techniques.

Experimental Section

General Methods. General experimental conditions, absorbance measurements in the UV−Visible region, viscometric determinations, and molecular modeling studies were carried out as described previously.[10e,27] Compounds **1** and **6** were prepared as described previously.[27]

Synthesis of *N*-Amino-γ-carboliniums 2 and 7. General Procedure. To a suspension of the γ-carboline **1** (1 mmol) in CH_2Cl_2 (5 mL) was slowly added a solution of *O*-hydroxylamino mesitylenesulfonate (MSH)[39] (0.26 g, 1.2 mmol) in CH_2Cl_2 (5 mL). The reaction mixture was stirred at room temperature overnight. The precipitate formed was isolated by filtration and recrystallized from the appropriate solvent.

2-Amino-1-methyl-5*H*-pyrido[4,3-*b*]indol-2-inium Mesitylenesulfonate (2a). Yield: 77%. Mp: 227−228 °C (white powder from EtOAc/EtOH). IR (KBr): υ_{max} 3272, 3084, 1639, 1608, 1458, 1197, 1086 cm^{-1}. ^1H NMR (DMSO-d_6): δ 13.04 (bs, 1H, NH); 8.58 (d, 1H, J = 7.0 Hz); 8.38 (d, 1H, J = 8,1 Hz); 7.83 (d, 1H, J = 7.0 Hz); 7.77 (d, 1H, J = 8.4 Hz); 7.67 (t, 1H, J = 8.4 Hz, J = 7.0 Hz); 7.47 (t, 1H, J = 8,1 Hz, J = 7.0 Hz); 7.37 (s, 2H, NH_2); 6,70 (s, 2H); 3,21 (s, 3H); 2.47 (s, 6H); 2.13 (s, 3H) ppm. MS (EI) *m*/*z* (rel int.): 197 (M^+, 43); 182 (100); 154 (28); 117 (43); 91 (37). Anal. Calcd for $C_{21}H_{23}N_3O_3S$ (397.49): C, 63.46; H, 5,83; N, 10,57. Found: C, 63.16; H, 5,58; N, 10,43.

2-Amino-1,3-dimethyl-5*H*-pyrido[4,3-*b*]indol-2-inium Mesitylenesulfonate (2b). Yield: 93%. Mp: 256−257 °C (white powder from EtOAc/EtOH). IR (KBr): υ_{max} 3293, 3171, 1639, 1612, 1459, 1174, 1085 cm^{-1}. ^1H NMR (DMSO-d_6): δ 12.85 (bs, 1H, NH); 8.33 (d, 1H, J = 8.1 Hz); 7.77 (s, 1H); 7.72 (d, 1H, J = 8.1 Hz); 7.65 (t, 1H, J = 8.1 Hz, J = 7.0 Hz); 7.47 (t, 1H, J = 8.1 Hz, J = 7.0 Hz); 7.37 (s, 2H, NH_2); 6.69 (s, 2H); 3,25 (s, 3H); 2.82 (s, 3H); 2.47 (s, 6H); 2.12 (s, 3H) ppm. MS (EI) *m*/*z* (rel int.): 196 (100); 117 (28). Anal. Calcd for $C_{22}H_{25}N_3O_3S$ (411.52): C, 64.21; H, 6.12; N, 10.21. Found: C, 64.50; H 6.37; N, 10.43.

2-Amino-1,7,8-trimethyl-5*H*-pyrido[4,3-*b*]indol-2-inium Mesitylenesulfonate (2c). Yield: 92%. Mp: 275−276 °C (white powder from EtOAc/EtOH). IR (KBr): υ_{max} 3272, 1614, 1468, 1184, 1086 cm^{-1}. ^1H NMR (DMSO-d_6): δ 12.65 (bs, 1H, NH); 8.52 (d, 1H, J = 7.0 Hz); 8.13 (s, 1H); 7.75 (d, 1H, J = 7.0 Hz); 7.54 (s, 1H); 7.32 (s, 2H, NH_2); 6,70 (s, 2H); 3.19 (s, 3H); 2.47 (s, 6H); 2.42 (s, 6H); 2.13 (s, 3H) ppm. MS (EI) *m*/*z* (rel int.): 210 (100); 195 (47); 117 (35); 105 (36). Anal. Calcd for $C_{23}H_{27}N_3O_3S$ (425.55): C, 64.92; H, 6.39; N, 9,87. Found: C, 64.80; H, 6.25; N, 10.02.

2-Amino-1,3,7,8-tetramethyl-5*H*-pyrido[4,3-*b*]indol-2-inium Mesitylenesulfonate (2d). Yield: 89%. Mp: 272−273 °C (white powder from EtOH). IR (KBr): υ_{max} 3313, 1627, 1468, 1222, 1167, 1082 cm^{-1}. ^1H NMR (DMSO-d_6): δ 12.62 (bs, 1H, NH); 8,09 (s, 1H); 7.69 (s, 1H); 7.49 (s, 1H); 6,70 (s, 2H); 6.64 (s, 2H, NH_2); 3,21 (s, 3H); 2.79 (s, 3H); 2.47 (s, 6H); 2.41 (s, 6H); 2.13 (s, 3H) ppm. MS (EI) *m*/*z* (rel int.): 224 (100); 209 (29); 117 (21). Anal. Calcd for $C_{24}H_{29}N_3O_3S$ (439.57): C, 65.58; H, 6.65; N, 9.56. Found: C, 65.12; H, 7.01; N, 9.32.

5-Amino-6,8,9-trimethyl-11*H*-indolo[3,2-*c*]quinolin-5-inium Mesitylenesulfonate (7). Yield: 66%. Mp: 266−267 °C (white powder from EtOH). IR (KBr): υ_{max} 3279, 3169, 1590, 1541, 1470, 1209, 1167, 1085 cm^{-1}. ^1H NMR (DMSO-d_6): δ 13.79 (bs, 1H, NH); 8.72 (d, 2H, J = 8.3 Hz); 8.18 (s, 1H); 8.09 (t, 1H, J = 8.3 Hz, J = 7.3 Hz); 7.96 (t, 1H, J = 8.3 Hz, J = 7.3 Hz); 7.64 (s, 1H); 6,96 (s, 2H, NH_2); 6.69 (s, 2H); 3.45 (s, 3H); 2.47 (s, 6H); 2.46 (s, 6H); 2.13 (s, 3H) ppm. MS (EI) *m*/*z* (rel int.): 260 (100); 245 (31); 117 (53). Anal. Calcd for $C_{27}H_{29}N_3O_3S$ (475.61): C, 68.19; H, 6.15; N, 8.84. Found: C, 68.35; H, 6.08; N, 8.72.

Synthesis of Compounds 3. General Procedure. A mixture of *N*-amino-γ-carbolinium **2** (1 mmol), 2,3-butanedione or 3,4-hexanedione (1.1 mmol), Et_3N (0.15 mL, 1.1 mmol), acetone (6 mL), and MeOH (6 mL) was heated at reflux for 3−8 h. The solvent was evaporated under reduced pressure, and the residue was triturated with acetone. The solid obtained was isolated by filtration and recrystallized from the appropriate solvent to give pure salts **3a**−**e**. For **3f** the reaction was carried out in EtOH (6 mL) and Bu_2NH (0.25 mL) was used instead of Et_3N. The reaction mixture was refluxed for 6 h and worked up as indicated above.

2,3-Dimethyl-8*H*-pyridazino[1′,6′:1,2]pyrido[4,3-*b*]indol-5-inium Mesitylenesulfonate (3a). Yield: 75%. Mp: 283−284 °C (cream color powder from EtOH). IR (KBr): υ_{max} 3428, 1637, 1604, 1404, 1169, 1083 cm^{-1}. ^1H NMR (DMSO-d_6): δ 13.30 (bs, 1H, NH); 9,28 (d, 1H, J = 7.3 Hz); 9,22 (s, 1H); 8,88 (d, 1H, J = 8.2 Hz); 8.27 (d, 1H, J = 7.3 Hz); 7.91 (d, 1H, J = 8.2 Hz); 7.74 (t, 1H, J = 8.2 Hz, J = 7.3 Hz); 7.58 (t, 1H, J = 8.2 Hz, J = 7.3 Hz); 6,73 (s, 2H); 2.75 (s, 3H); 2.72 (s, 3H); 2.49 (s, 6H); 2.16 (s, 3H) ppm. MS (EI) *m*/*z* (rel int.): 247 (M^+, 100); 205 (26). Anal. Calcd for $C_{25}H_{25}N_3O_3S$ (447.55): C, 67.09; H, 5.63; N, 9.39. Found: C, 66.81; H, 5.80; N, 9.64.

2,3,6-Trimethyl-8*H*-pyridazino[1′,6′:1,2]pyrido[4,3-*b*]indol-5-inium Mesitylenesulfonate (3b). Yield: 71%. Mp: 267−268 °C (cream color from EtOH). IR (KBr): υ_{max} 3428, 1639, 1609, 1407, 1166, 1085 cm^{-1}. ^1H NMR (DMSO-d_6): δ 13,20 (bs, 1H, NH); 9,20 (s, 1H); 8,84 (d, 1H, J = 8,0 Hz); 8.28 (s, 1H); 7.84 (d, 1H, J = 7.9 Hz); 7.71 (t, 1H, J = 7.9 Hz, J = 7,2 Hz); 7.54 (t, 1H, J = 8.0 Hz, J = 7.2 Hz); 6.71 (s, 2H); 3.01 (s, 3H); 2.77 (s, 3H); 2.72 (s, 3H); 2.49 (s, 6H); 2.14 (s, 3H) ppm. Anal. Calcd for $C_{26}H_{27}N_3O_3S$ (461.58): C, 67.66; H, 5.90; N, 9.10. Found: C, 67.42; H, 5.95; N, 9.35.

2,3,6,10,11-Pentamethyl-8*H*-pyridazino[1′,6′:1,2]pyrido-[4,3-*b*]indol-5-inium Mesitylenesulfonate (3c). Yield: 63%. Mp: 315−316 °C (yellow powder from EtOH). IR (KBr): υ_{max} 3430, 1642, 1615, 1432, 1185, 1086 cm^{-1}. ^1H NMR (DMSO-d_6): δ 12.95 (bs, 1H, NH); 9,06 (s, 1H); 8.51 (s, 1H); 8.16 (s, 1H); 7.58 (s, 1H); 6,71 (s, 2H); 2.97 (s, 3H); 2.74 (s, 3H); 2.70 (s, 3H); 2.47 (s, 12H); 2.14 (s, 3H) ppm. MS (EI) *m*/*z* (rel int.): 290 (M^+,21); 289 (100); 117 (23). Anal. Calcd for $C_{28}H_{31}N_3O_3S$ (489,63): C, 68.69; H, 6.38; N, 8.58. Found: C, 68.45; H, 6.22; N, 8.61.

(39) Tamura, Y.; Minamikawa, J.; Ikeda, M. *Synthesis* **1977**, 1.

2,3-Diethyl-8*H*-pyridazino[1′,6′:1,2]pyrido[4,3-*b*]indol-5-inium Mesitylenesulfonate (3d). Yield: 82%. Mp: 243−244 °C (cream color powder from EtOH/EtOAc). IR (KBr): υ_{max} 3448, 1632, 1602, 1402, 1164, 1082 cm^{-1}. ^{1}H NMR (DMSO-d_6): δ 13,25 (bs, 1H, NH); 9.27 (d, 1H, J = 7.2 Hz); 8.99 (s, 1H); 8.75 (d, 1H, J = 8.1 Hz); 8.25 (d, 1H, J = 7,2 Hz); 7.88 (d, 1H, J = 8.1 Hz); 7.73 (t, 1H, J = 8.1 Hz, J = 7.3 Hz); 7.57 (t, 1H, J = 8.1 Hz, J = 7.3 Hz); 6.70 (s, 2H); 3.15 (c, 2H, J = 7.3 Hz); 3.05 (c, 2H, J = 7.3 Hz); 2.48 (s, 6H); 2.14 (s, 3H); 1.41 (t, 6H, J = 7.3 Hz) ppm. MS (EI) *m*/*z* (rel int.): 276 (M$^+$,19); 275 (100); 117 (41). Anal. Calcd for $C_{27}H_{29}N_3O_3S$ (475.61): C, 68.19; H, 6.14; N, 8.84. Found: C, 68.06; H, 6.22; N, 8.84.

2,3-Diethyl-6-methyl-8*H*-pyridazino[1′,6′:1,2]pyrido-[4,3-*b*]indol-5-inium Mesitylenesulfonate (3e). Yield: 76%. Mp: 228−229 °C (cream color powder from EtOH/ EtOAc). IR (KBr): υ_{max} 3447, 1641, 1606, 1404, 1163, 1083 cm^{-1}. ^{1}H NMR (DMSO-d_6): δ 13.20 (bs, 1H, NH); 9.04 (s, 1H); 8.76 (d, 1H, J = 8.1 Hz); 8.30 (s, 1H); 7.86 (d, 1H, J = 8.2 Hz); 7.72 (t, 1H, J = 8.2 Hz, J = 7.3 Hz); 7.56 (t, 1H, J = 8.1 Hz, J = 7.3 Hz); 6.71 (s, 2H); 3,20 (c, 2H, J = 7.3 Hz); 3.09−3.06 (m, 5H); 2.48 (s, 6H); 2.14 (s, 3H); 1.47−140 (m, 6H) ppm. MS (EI) *m*/*z* (rel int.): 290 (M$^+$, 22); 289 (100). Anal. Calcd for $C_{28}H_{31}N_3O_3S$ (489.64): C, 68.69; H, 6.38; N, 8.58. Found: C,68.51; H, 6.25; N, 8.72.

2,3-Diethyl-6,10,11-trimethyl-8*H*-pyridazino[1′,6′:1,2]-pyrido[4,3-*b*]indol-5-inium Mesitylenesulfonate (3f). Yield: 72%. Mp: 294−295 °C (yellow powder from EtOH). IR (KBr): υ_{max} 3439, 1637, 1612, 1403, 1180, 1084 cm^{-1}. ^{1}H NMR (DMSO-d_6): δ 13.05 (bs, 1H, NH); 8.96 (s, 1H); 8.45 (s, 1H); 8.20 (s, 1H); 7.61 (s, 1H); 6.71 (s, 2H); 3.20 (q, 2H, J = 7.3 Hz); 3.10−3.02 (m, 5H); 2.48 (s, 12H); 2.15 (s, 3H); 1.46−1.39 (m, 6H) ppm. MS (EI): *m*/*z* (rel int.): 318 (M$^+$, 24); 317 (100); 117 (37). Anal. Calcd for $C_{30}H_{35}N_3O_3S$ (517.69): C, 69.60; H, 6.81; N, 8.12. Found: C, 69.30; H, 7.06; N, 8.08.

Synthesis of Compounds 4 and 5. General Procedure. A mixture of *N*-amino-γ-carbolinium **2** (1 mmol), 1,2-acenaphthenequinone or 9,10-phenanthrenequinone (1.1 mmol), NaOAc (90 mg, 1.1 mmol), and acetone (10 mL) was heated at reflux for 2−3 h. The precipitate formed was filtered, washed with water, and recrystallized from the appropriate solvent.

13*H*-Dibenz[*f*,*h*]indolo[3′,2′:3,4]pyrido[1,2-*b*]cinnolin-10-inium Mesitylenesulfonate (4). Yield: 74%. Mp: 335−336 °C (red prisms from EtOH). IR (KBr): υ_{max} 3433, 1614, 1601, 1388, 1174, 1120 cm^{-1}. ^{1}H NMR (DMSO-d_6): δ 16.54 (bs, 1H, NH); 10.03 (s, 1H); 9.60 (d, 1H, J = 7.1 Hz); 9.30 (d, 1H, J = 8.3 Hz); 9.12−9.08 (m, 2H); 8.80−8.76 (m, 2H); 8.46 (d, 1H, J = 7.3 Hz); 7.96−7.83 (m, 5H); 7.75 (t, 1H, J = 8.3 Hz, J = 7.3 Hz); 7.62 (t, 1H, J = 8.3 Hz, J = 7.3 Hz); 6.71 (s, 2H); 2.48 (s, 6H); 2.14 (s, 3H) ppm. Anal. Calcd for $C_{35}H_{27}N_3O_3S$ (569.68): C, 73.79; H, 4.78; N, 7.38. Found: C, 73.55; H, 4.88; N, 7.44.

5*H*-Acenaphtho[1″,2″:3′,4′]pyridazino[1′,6′:1,2]pyrido-[4,3-*b*]indole-8-inium Mesitylenesulfonate (5a). Yield: 81%. Mp: 338−339 °C (yellow powder from EtOH). IR (KBr): υ_{max} 3439, 1604, 1497, 1419, 1175, 1085 cm^{-1}. ^{1}H NMR (DMSO-d_6): δ 16.80 (bs, 1H, NH); 9.80 (s, 1H); 9.43 (d, 1H, J = 7.5 Hz); 9.03 (d, 1H, J = 8.1 Hz); 8.91 (d, 1H, J = 6.8 Hz); 8.47 (d, 1H, J = 7.3 Hz); 8.36 (d, 1H, J = 8.1 Hz); 8.32 (d, 1H, J = 8.3 Hz); 8.28 (d, 1H, J = 7.5 Hz); 8.03−7.96 (m, 2H); 7.86 (d, 1H, J = 8.1 Hz); 7.72 (t, 1H, J = 8.1 Hz, J = 7.2 Hz); 7.59 (t, 1H, J = 8.1 Hz, J = 7.2 Hz); 6.72 (s, 2H); 2.47 (s, 6H); 2.13 (s, 3H) ppm. Anal. Calcd for $C_{33}H_{25}N_3O_3S$ (543.65): C, 72.91; H, 4.63; N, 7.73. Found: C, 72.65; H, 4.49; N, 7.71.

2,3,7-Trimethyl-5*H*-acenaphtho[1″,2″:3′,4′]pyridazino-[1′,6′:1,2]pyrido[4,3-*b*]indol-8-inium Mesitylenesulfonate (5b). Yield: 83%. Mp: >350 °C (yellow powder from EtOH). IR (KBr): υ_{max} 3442, 1618, 1514, 1420, 1171, 1081 cm^{-1}. ^{1}H NMR (DMSO-d_6): δ 16.40 (bs, 1H, NH); 9.57 (s, 1H); 8.88 (d, 1H, J = 7.3 Hz); 8.57 (s, 1H); 8.45 (d, 1H, J = 7.1 Hz); 8.37 (d, 1H, J = 8.2 Hz); 8.32 (d, 1H, J = 8.4 Hz); 8.16 (s, 1H); 8.03−7.97 (m, 2H); 7.44 (s, 1H); 6.72 (s, 2H); 3.13 (s, 3H); 2.49 (s, 6H); 2.39 (s, 6H); 2.14 (s, 3H) ppm. Anal. Calcd for $C_{36}H_{31}N_3O_3S$ (585.72): C, 73.82; H, 5.33; N, 7.17. Found: C, 74.05; H, 5.45; N, 7.06.

2,3-Diethyl-12,13-dimethyl-10*H*-indolo[3,2-*c*]pyridazino-[1,6-*a*]quinolin-5-inium Mesitylenesulfonate (8). Yield: 73%. Mp: 270−271 °C (yellow powder from EtOH). IR (KBr): υ_{max} 3428, 1634, 1588, 1456, 1228, 1169 cm^{-1}. ^{1}H NMR (DMSO-d_6): δ 14.20 (bs, 1H, NH); 9.20 (d, 1H, J = 8.1 Hz); 8.97 (s, 1H); 8.78 (d, 1H, J = 8.4 Hz); 8.40 (s, 1H); 8.16−8.09 (m, 2H); 7.64 (s, 1H); 6.72 (s, 2H); 3,25 (q, 2H, J = 7.3 Hz); 3.13 (q, 2H, J = 7.3 Hz); 2.48 (s, 12H); 2.14 (s, 3H); 1.54 (t, 1H, J = 7.3 Hz); 1.45 (t, 1H, J = 7.3 Hz) ppm. Anal. Calcd for $C_{33}H_{35}N_3O_3S$ (517.69): C, 71.58; H, 6.38; N, 7.59. Found: C, 71.48; H, 6.53; N, 7.48.

Synthesis of hHeterobetaines 9a and 11a. General Procedure. To a suspension of the azonia derivative **3a** or **5a** (1 mmol) in CH_2Cl_2 (25 mL) was added dried K_2CO_3 (1.38 g, 10 mmol), and the mixture was stirred at room temperature for 2 h. The resulting suspension was filtered under vacuum, and the solid was washed with CH_2Cl_2 until complete decoloration. The organic filtrates were concentrated under reduced pressure, and the solid residue obtained was recrystallized from the appropriate solvent.

2,3-Dimethylpyridazino[1′,6′:1,2]pyrido[4,3-*b*]indole (9a). Yield: 90%. Mp: 260−261 °C (yellow powder from CH_3CN). IR (KBr): υ_{max} 1639, 1618, 1589, 1398, 1222 cm^{-1}. ^{1}H NMR (DMSO-d_6): δ 8.84 (s, 1H); 8.74 (d, 1H, J = 7.5 Hz); 8.61 (d, 1H, J = 7.7 Hz); 7.84 (d, 1H, J = 7.5 Hz); 7.78 (d, 1H, J = 8.1 Hz); 7.50 (t, 1H, J = 8.1 Hz, J = 7.0 Hz); 7.30 (t, 1H, J = 7.7 Hz, J = 7.0 Hz); 2.58 (s, 3H); 2.55 (s, 3H) ppm. MS (EI) *m*/*z* (rel int.): 247 (M$^+$, 100); 205 (37). Anal. Calcd for $C_{16}H_{13}N_3$ (247.30): C, 77.71; H, 5.30; N, 16.99. Found: C, 77.85; H, 5.20; N, 16.78.

Acenaphtho[1″,2″:3′,4′]pyridazino[1′,6′:1,2]pyrido[4,3-*b*]indole (11a). Yield: 90%. Mp: 325−326 °C (red prisms from EtOH) IR (KBr): υ_{max} 1614, 1589, 1396, 1228 cm^{-1}. ^{1}H NMR (DMSO-d_6): δ 9.75 (s, 1H); 9.16 (d, 1H, J = 7.0 Hz); 8.99 (d, 1H, J = 7.7 Hz); 8.90 (d, 1H, J = 7.3 Hz); 8.44 (d, 1H, J = 7.0 Hz); 8.36−8.30 (m, 2H); 8.07−7.93 (m, 3H); 7.85 (d, 1H, J = 8.1 Hz); 7.62 (t, 1H, J = 8.1 Hz, J = 7.0 Hz); 7.47 (t, 1H, J = 7.7 Hz, J = 7.0 Hz) ppm. Anal. Calcd for $C_{24}H_{13}N_3$ (343.39): C, 83.95; H, 3.84; N, 12.24. Found: C, 83.73; H, 3.92; N, 12.35.

DNA Binding Experiments. Calf Thymus DNA for viscosity and spectrophotometric binding analysis was purchased from Sigma Chemical Co. DNA concentrations were determined by absorbance measurements by using an extinction coefficient of 6600 M^{-1} cm^{-1} at 260 nm and are expressed in terms of nucleotide equivalents per liter. The aqueous buffer used was TRIS buffer (50 mM TRIS, 15 mM NaCl, pH= 7.6).

UV−Visible Spectrophotometric Studies. All compounds examined obeyed Beer's law over the range of concentrations used (0−20 μM), and the molar extinction coefficients were determined at their appropriate λ_{max} values by Beer's law plots. Molar extinction coefficients of compounds bound to DNA were determined at the same wavelength as the molar extinction coefficient measurements of the free compound, but a larger molar excess of DNA was present ([DNA nucleotides]/[compound] > 20−100). Spectrophotometric titrations were performed by serial addition of 50−100 μL aliquots of a DNA stock solution (0.1−0.5 mM DNA nucleotides in TRIS buffer) into a 10 cm path length quartz cell containing a dilute compound solution (6−20 μM) in the same buffer and scanning the UV−vis spectrum after each addition. Titrations were stopped when no shift to the lower energy range of the maximum absorbance wavelength in the spectrum was detected between additions. These absorbance values were converted to υ (moles of bound compound/moles of DNA nucleotides) and c (free ligand concentrations) using the free and bound molar extinction coefficients for the analyzed compound. Experimental data which were in the fraction bound range 0.2 to 0.8 (results outside of this range are subject to large systematic errors as a result of experimental errors in molar extinction coefficient determinations[40]) were plotted using the method of Scatchard. The salts **3** were analyzed by the extended neighbor-exclusion model of McGhee and von Hippel[32] using a nonlinear least-squares fitting procedure to derive the binding parameters (K, n) with a computer program[41] from the following equation:

$$v/c = K(1 - nv)[(1 - nv)/(1 - (n - 1)v)]^{n-1}$$

Viscometric Measurements. Samples of DNA (3 mg/mL) in a 0.01 M (pH = 6.9) phosphate buffer were prepared and sonicated as described by Davidson.[42] The average molecular weight of the fragments produced after sonication was determined to be 3.6×10^5 daltons by viscometric analysis, as described by Eigner and Doty.[43] The purified sonicated DNA sample displayed an A_{260}/A_{280} ratio of between 1.88 and 1.93 and a total hyperchromicity at 260 nm of 30%.

The viscometric titrations were performed in a capillary viscometer at 25 ± 0.01 °C. At least four flow times were used to calculate the average relative viscosity for each DNA solution. If any readings differed by more than 0.03 s, further measurements were made. Reduced specific viscosity was calculated by the method of Cohen and Eisenberg.[34] For each compound, 2−4 experiments were carried out. The value of L/L_o was plotted for each experiment as a function of r. The lines passing through the experimental points were fitted by the least-squares method and forced to pass through the origin.

Unwinding Angle Determination. The unwinding angle determinations were performed using the viscometric method of Revet[36c] and were measured with closed circular DNA from pBR325 plasmid (Sigma Chemical Co.). Conditions were the same as those for the linear DNA titrations.

Acknowledgment. We thank the Comisión Interministerial de Ciencia y Tecnología (CICYT, project SAF98-0093) and Comunidad Autónoma de Madrid (project AE00159/95) for financial support, and studentships (A.M. and B.P.T.) from the Ministerio de Educación y Ciencia are gratefully acknowledged.

JO982216D

(40) Deranleau, D. A. *J. Am. Chem. Soc.* **1969**, *91*, 4044.
(41) Hintze, J. L. BMPD Statistical Sofware Inc.. Los Angeles, CA, 1991.
(42) Davidson, M. W.; Griggs, B. G.; Boykin, D. W.; Wilson, W. D. *J. Med. Chem*. **1977**, *20*, 1117.
(43) Eigner, J.; Doty, P. *J. Mol. Biol*. **1965**, *12*, 549.